U-PB DATING OF SUBSURFACE PYROCLASTIC DEPOSITS (TAHORAKURI FORMATION) AT NGATAMARIKI AND ROTOKAWA GEOTHERMAL FIELDS

Alan A. Eastwood[1], Darren M. Gravley[1], Colin J. N. Wilson[2], Isabelle Chambefort[3], Christopher Oze[1], Jim W. Cole[1], Trevor R. Ireland[4]

[1]Department of Geological Sciences, University of Canterbury, Private Bag 4800, Christchurch 8140, New Zealand

[2]School of Geography, Environment and Earth Sciences, Victoria University of Wellington, PO Box 600, Wellington 6140, New Zealand

[3]GNS Science, Wairakei Research Centre, Taupo 3384, New Zealand

[4]Research School of Earth Sciences, Australian National University, Canberra, ACT 0200, Australia

alan.eastwood@pg.canterbury.ac.nz

Keywords: *U-Pb dating, zircon, Tahorakuri Formation, Ngatamariki, Rotokawa, Taupo Volcanic Zone*

ABSTRACT

We present secondary ion mass spectrometry (SIMS) U-Pb age data and crystallisation-age spectra for zircons from altered pyroclastic rocks penetrated by drillholes at the Ngatamariki and Rotokawa geothermal fields, Taupo Volcanic Zone (TVZ), New Zealand. These rocks form part of the Tahorakuri Formation, which includes the oldest silicic deposits in the TVZ and therefore provides valuable insights into early TVZ history. The age spectra are used to estimate eruption ages, with the oldest two estimated at 1.89 ± 0.02 Ma (95% confidence limits) and 1.88 ± 0.03 Ma; 200-300 ka older than the oldest exposed silicic deposits from the TVZ. Samples at 0.915 ± 0.055 Ma and 0.873 ± 0.031 Ma most likely correlate to the Akatarewa ignimbrite, previously recorded at nearby geothermal fields. The youngest units at 0.806 ± 0.032 Ma and 0.701 ± 0.039 Ma, and were followed by a long period with no large-scale explosive volcanism until the Whakamaru-group ignimbrites at ~350 ka. A large buried andesite volcano at Rotokawa is >1.89 Ma in age, indicating that andesitic volcanism of this age was not restricted to the western margin of the TVZ as has previously been suggested. Rifting within TVZ appears to have begun prior to ~1.9 Ma, as shown by significant basin development that occurred prior to the emplacement of the oldest silicic deposits. These results indicate that silicic volcanism within the TVZ may have begun earlier than previously thought.

1. INTRODUCTION

The rock core and cuttings samples recovered from geothermal drilling provide evidence as to the nature of the subsurface stratigraphy that is often not available from surficial exposures. This can provide valuable insight into the geological history of a region, particularly in an actively rifting environment such as the Taupo Volcanic Zone (TVZ), New Zealand. Here, the oldest deposits are deeply buried due to subsidence resulting from rifting, and burial by younger deposits. In particular, the voluminous Whakamaru-group ignimbrites erupted at ~350 ka (Leonard et al., 2010) are a widespread marker plane that conceals older deposits throughout much of the central North Island.

A major challenge in using geothermal drilling records for correlation is that high-temperature fluids circulating within the geothermal systems can alter distinctive chemical, mineralogical, and textural characteristics, making correlation of units extremely difficult. Most of the pre-Whakamaru rock sequence in many TVZ geothermal fields is, therefore, lumped into the Tahorakuri Formation (Gravley et al., 2006; Chambefort et al., 2013). Within the TVZ, early correlations of units were based on mineralogy and petrographic characteristics, or sometimes chemical characteristics (e.g. Bignall et al., 1996). However, there is uncertainty as to the utility of this approach in strongly altered rocks typical of those at depth within geothermal fields. Existing U-Pb zircon dating shows that many previous correlations are inaccurate (Wilson et al., 2010).

Here we report U-Pb age data for intervals within the Tahorakuri Formation from the Ngatamariki and Rotokawa geothermal fields (Figure 1). These data help to establish a chronostratigraphy for the southern part of the central TVZ, providing valuable insight into volcanic activity and rifting during the early stages of the TVZ.

2. GEOLOGICAL SETTING

The TVZ (Figure 1) is a rifted arc resulting from the oblique subduction of the Pacific Plate beneath the North Island of New Zealand. The eastern part of the North Island is rotating clockwise as a series of discrete tectonic blocks, resulting in rifting within the TVZ (Wallace et al., 2004). At the surface, this extension is expressed as a NNE-SSW trending system of normal faults commonly referred to as the Taupo Rift (Villamor and Berryman, 2006).

Andesitic volcanic activity in the TVZ is considered to have begun at ~2 Ma, with silicic volcanism from ~1.6 Ma (Houghton et al., 1995; Wilson et al., 1995). The oldest andesitic cones are exposed along the western TVZ margin, with Hauhungaroa, Titiraupenga and Pureora (Figure 1) dated at ~2.0 Ma, 1.89 Ma and 1.60 Ma, respectively (Graham et al., 1995; Leonard et al., 2010). The earliest known silicic activity originated from Mangakino caldera in what Wilson et al. (1995) term the 'old TVZ' (>0.34 Ma). The Whakamaru-group ignimbrites mark the boundary between the 'old TVZ' and the 'young TVZ' (<0.34 Ma to present; Wilson et al., 1995). Surface exposures of pre-Whakamaru volcanic deposits are mainly located to the west of the currently active TVZ (Leonard et al., 2010). Distinct segmentation of the TVZ is present, with andesitic volcanism dominating in the northern and southern sections, and voluminous rhyolitic volcanism in the central section associated with eight partially delineated calderas (Wilson et al., 2009). There are 23 active high-temperature geothermal systems in the TVZ, most of which are located to the east of the Taupo Rift (Bibby et al., 1995).

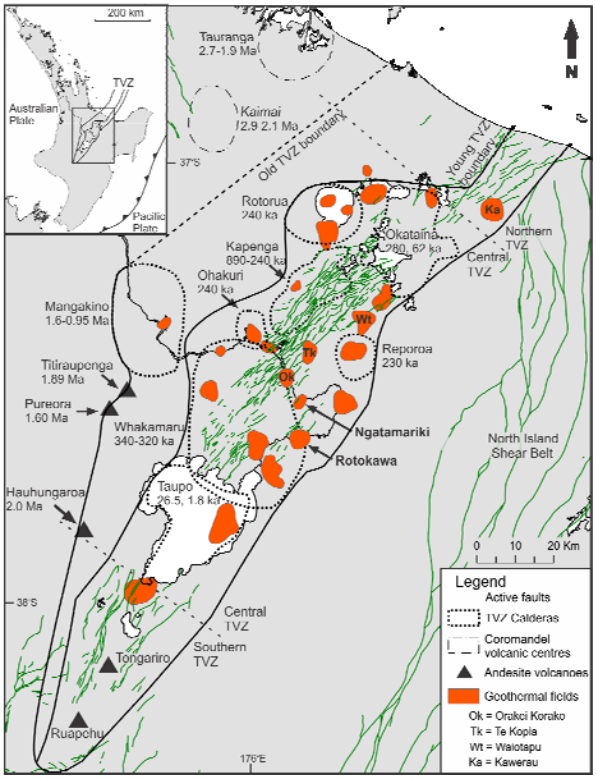

Figure 1: Map of the TVZ. Old (1.6 Ma to 350 ka) and young (350 ka to present) boundaries and calderas are from Wilson et al. (2009). Coromandel volcanic centres (from Briggs et al., 2005), geothermal fields (from Bibby et al., 1995), and active faults (from Townsend et al., 2008; Leonard et al., 2010; Lee et al., 2011) are also shown. Ages for andesite cones are from Graham et al. (1995) and Leonard et al. (2010).

Ngatamariki Geothermal Field (Figure 2) is located ~17 km NE of Taupo township, and just outside the eastern margin of the Whakamaru caldera proposed by Wilson et al. (1986). Surface activity associated with the Ngatamariki geothermal system is relatively minor (Bignall, 2009) and the full extent of the field has been established from subsurface geophysical data. There is a shallow low resistivity anomaly associated with hydrothermal alteration south of the Waikato River and the hydrothermal system extends further to the south at depth (Urzúa-Monsalve, 2008). The NE-SW trending surface faults (Figure 2) reflect the regional structure of the TVZ. The Aratiatia Fault passes just south of well NM6, with Rotokawa located further south.

3. SUBSURFACE STRATIGRAPHY

3.1 Ngatamariki

The overall stratigraphy at Ngatamariki is described in Chambefort et al. (2013) and shown in Figure 3. Pre-Whakamaru deposits within the geothermal fields of the central TVZ have been collectively termed the Reporoa Group (Gravley et al., 2006). This group consists of: 1) the Tahorakuri Formation, including un-correlated volcanic, volcaniclastic, and sedimentary deposits; 2) the Waikora Formation, consisting of greywacke-rich gravels; and 3) named ignimbrites and lava flows at individual geothermal fields. At Ngatamariki, the Tahorakuri Formation can be divided into a sedimentary succession overlying a pyroclastic succession (Chambefort et al., 2013). The sedimentary succession is dominated by fine-grained siltstone to mudstone interbedded with minor pyroclastic deposits, interpreted to represent a lacustrine environment.

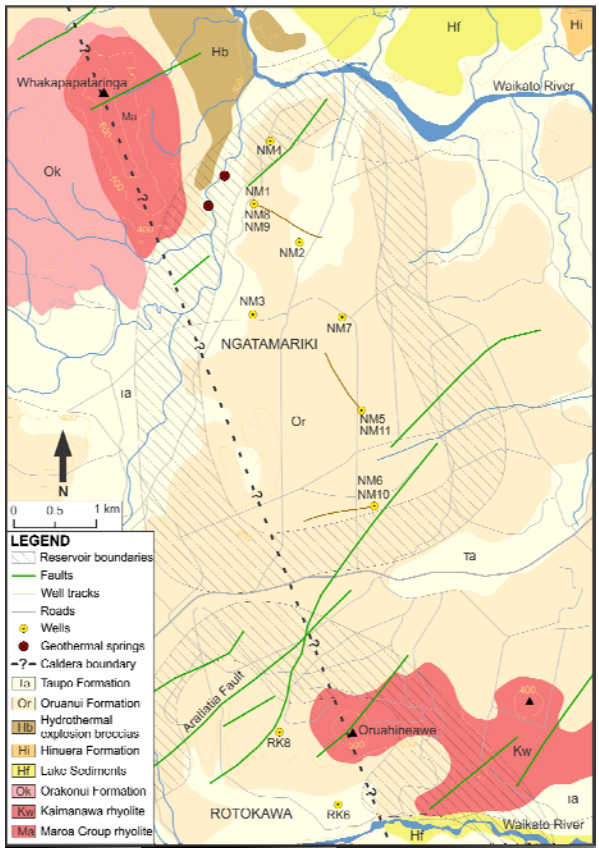

Figure 2: Map of Ngatamariki and the northern part of Rotokawa. Hatching indicates the approximate reservoir boundaries for Ngatamariki (from Boseley et al., 2010) and Rotokawa (from Risk, 2000). Geological formations and active faults are from Leonard et al. (2010).

The Tahorakuri Formation pyroclastic succession contains wide variations; however, intense alteration and the fine grainsize of the drill cuttings makes correlations complex. The upper part of the succession is dominated by intensely altered, crystal-poor (10-15%) deposits with minor plagioclase pseudomorphs, very rare (<<1%), small (mostly <0.3 mm) quartz fragments and completely altered ferromagnesian minerals. Welding textures are only sometimes preserved, and imply that one or more welded ignimbrites are present towards the top of this succession (Figure 3). Below, and sometimes also above the welded ignimbrites, the succession is characterized by strongly altered volcaniclastic deposits with no visible primary textures and minor volumes of crystal pseudomorphs.

Below the intensely altered volcaniclastic deposits, another welded ignimbrite can be recognized in some wells. This ignimbrite contrasts with the shallower one due to its higher crystal content (20-30%). Here quartz is also more common (>1%) and phenocrysts are generally larger (mostly >0.5 mm) and sometimes embayed. Based on geochemical similarities, Bignall et al. (1996) suggested this is the Akatarewa ignimbrite, an ignimbrite encountered in nearby geothermal fields, and U-Pb dated at 0.95 ± 0.05 Ma at Orakei Korako and Te Kopia (Wilson et al., 2010).

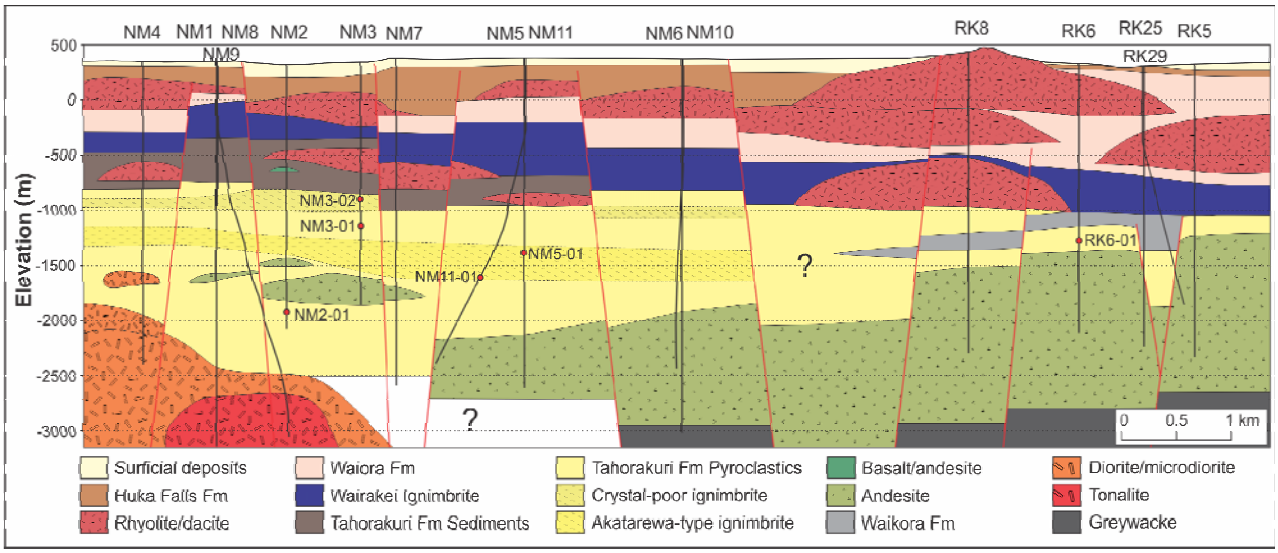

Figure 3: Simplified cross section showing the subsurface stratigraphy at Ngatamariki and Rotokawa modified after Chambefort et al. (2013) and Rae (2007).

Below the Akatarewa ignimbrite the cuttings become extremely fine grained. Two core samples of the Tahorakuri Formation examined are both relatively crystal-rich (>20%) when compared to the shallower Tahorakuri material, but varying mineralogies indicate that multiple lithologies may be present. The deepest rock units also differ between the northern and southern parts of Ngatamariki. A thick sequence of andesite lava is encountered in the southern wells, and is interpreted to represent the northern margin of the andesite found at Rotokawa (Anderson, 2011). Diorite and tonalite plutons have been encountered at depth in the northern wells (Browne et al., 1992; Arehart et al., 2002; Chambefort et al., 2013), while the greywacke basement has also been encountered in NM6.

3.2 Rotokawa

The shallow stratigraphy encountered at Rotokawa is similar to Ngatamariki, but differs notably at depth. Here, most of the pre-Whakamaru sequence consists of andesite (Browne et al., 1992; Rae, 2007). This andesite rests on the greywacke basement, and likely formed a large composite cone volcano, with the northern margins reaching as far as the southern Ngatamariki wells (Anderson, 2011). Overlying the andesite, but only present in some wells, is a thin (20-250 m) pyroclastic sequence of the Tahorakuri Formation (Rae, 2007). Also present in some wells is a thin (10-250 m) sequence of Waikora Formation gravels.

4. SAMPLES AND METHODS

4.1 Samples

Six samples of the Tahorakuri Formation were chosen for this study, five from Ngatamariki and one from Rotokawa. The deepest sample, NM2-01, is of a crystal-rich ignimbrite. Primary textures are poorly preserved, although relict welding textures are rarely visible. The mineralogy is distinct from all other units observed at Ngatamariki due to the abundance of large (>1 mm), often embayed quartz phenocrysts and relict biotite (Table 1). The extent of this unit is unknown due to complete loss of cuttings during drilling, but pyroclastic deposits extend ~550 m deeper in nearby NM8A and NM9 (Chambefort et al., 2013).

Two cores of the Akatarewa-type ignimbrite were sampled. Both are relatively crystal-rich (>20%) and quartz-rich (>1%) compared to the shallow pyroclastic succession, and are dominated by plagioclase. Sample NM11-01 is moderately welded, with common flattened pumice and lithics. Quartz is mostly relatively fine (<0.5 mm), and possible rare ferromagnesian minerals are completely altered. Sample NM5-01 appears more strongly welded, and also contains common flattened pumice and lithics. Quartz phenocrysts are larger (often >1 mm) and often embayed. Ferromagnesian minerals are completely altered, but based on shape, amphibole appears to dominate.

Table 1: Summary of samples chosen for zircon dating in this study.

Sample	Depth (mRF)	Depth (mRL)	Mineralogy	Description
NM2-01	2254.7 to 2255.2	–1926 to –1926.5	pl (A), qz (C), amp (R), bt (R), ± pyx?	Crystal-rich (40-45%) ignimbrite with large (up to 3 mm), often embayed quartz and vague welding textures
NM11-01	2083.0 to 2089.9	–1610 to –1616	pl (A), qz (M), ± amp/pyx?	Pumice-, crystal- and lithic-rich ignimbrite, with aligned, flattened pumice, and minor quartz fragments
NM5-01	1775 to 1778	–1384 to –1387	pl (C), qz (M), amp ± pyx (M)	Welded ignimbrite with large (>1 mm), rounded, often embayed quartz, pumice fiamme, and minor lithics
NM3-01	1495.7 to 1497.7	–1145.7 to – 1147.7	pl (M), qz (M), ± amp/pyx?	Crystal-poor volcaniclastic unit with mostly fine (<1 mm), quartz fragments, minor lithics, and altered pumice
NM3-02	1246 to 1248	–896 to –898	pl (M), qz (R) ± amp/pyx?	Crystal-poor welded ignimbrite with common elongate pumice fiamme, minor lithics, and rare, mostly fine quartz
RK6-01	1612 to 1614	–1275.4 to –1277.4	pl (A), pyx ± amp (R)	Welded ignimbrite with small, wispy pumice fiamme, minor lithics, and moderate crystal content lacking quartz

Depths of the samples are given in metres below the drilling rig floor (mRF) and relative to sea level (mRL). Mineralogy refers to estimates of the primary mineral phases, which in many cases are completely altered and identified based on shape. Abbreviations used are: pl = plagioclase; qz = quartz; pyx = pyroxene; amp = amphibole; bt = biotite; A = abundant (>20 %); C = common (10-20 %); M = minor (1-10 %); R = rare (<1 %).

Sample NM3-01 is intensely altered and no primary textures were observed. It has a moderate crystal content consisting of quartz and altered crystal pseudomorphs (most likely plagioclase), with minor lithics and pumice in a fine groundmass. Quartz is generally small (<0.3 mm), and appears to consist primarily of broken crystal fragments. Sample NM3-02 is of a welded ignimbrite, with common pumice fiamme. The mineralogy is characteristic of much of the shallow pyroclastic succession, with a crystal-poor nature (~10%) and very rare, mostly small (<0.3 mm) quartz phenocrysts. Although completely altered, the majority of the crystal pseudomorphs are interpreted to have been plagioclase.

Sample RK6-01 is also of a welded ignimbrite with small, highly attenuated fiamme, interpreted to reflect intense welding. The mineralogy is notable for the apparent lack of quartz, being dominated by plagioclase pseudomorphs, with rare, completely altered ferromagnesian minerals. It is relatively crystal-rich (~20-25%) compared to the shallow pyroclastic succession at Ngatamariki.

4.2 Sample preparation

Samples were roughly crushed and then ground in a ringmill, before sieving to yield a <250 µm size fraction. When possible, lithic clasts were removed during crushing in order to minimise inheritance. Heavy minerals were concentrated by density separation using lithium polytungstate and methylene iodide. Concentrates were rinsed in nitric acid to remove pyrite, and then magnetic minerals were removed by passing the samples through a Frantz magnetic separator. Zircons were hand-picked from the remaining concentrate material, mounted in epoxy resin, and polished to expose the cores of the grains. Mounts were imaged by cathodoluminescence (CL) on a JEOL 6610 Scanning Electron Microprobe using a Robinson Detector.

4.3 Analytical techniques for ion probe

Age determinations on zircons were made by Secondary Ion Mass Spectrometry (SIMS) techniques using the Sensitive High-Resolution Ion Microprobe - Reverse Geometry (SHRIMP-RG) in the Research School of Earth Sciences, Australian National University (ANU). Techniques used were similar to those described in Milicich et al. (2013). In order to minimise contamination by common Pb, the mounts were rinsed in detergent, petroleum spirits and HCl prior to gold coating for both CL imaging and ion probe analysis. The primary beam was rastered for 180 s on a 35 × 45 µm area prior to data acquisition in order to remove the gold coating and any possible surface contamination. Ions were sputtered from the zircons with a 3-4 nA primary O_2^- beam focused to a ~25 × 35 µm spot. The mass spectrometer was cycled through peaks corresponding to $^{90}Zr_2{}^{16}O$, ^{204}Pb, background, ^{206}Pb, ^{207}Pb, ^{208}Pb, ^{238}U, $^{232}Th^{16}O$ and $^{238}U^{16}O$, with a total analysis time of ~900 s. Extended count times were used for ^{206}Pb (30 s) and ^{207}Pb (20 s), and six scans were run through the mass sequence. The concentration standard used was SL13 (238 ppm U) and the age standard was R33 (420 Ma ID-TIMS age from: http://earth.boisestate.edu/isotope/analytical-capabilities/id-tims-u-pb). Data reduction was carried out using SQUID 2 (Version 1.51, Ludwig, 2009).

The zircon/melt partition coefficient is higher for U than for Th, therefore, an initial deficit of ^{230}Th occurs in zircon during crystallisation. This creates a temporal gap in the $^{230}Th/^{234}U$ secular equilibrium of the ^{238}U decay chain and an underestimation of the zircon crystallisation age. Using the measured Th and U concentrations and a whole rock Th/U value of 4.4, a correction factor was applied using $f = (Th/U_{zir})/(Th/U_{magma})$ (Schärer, 1984).

The young age of the zircons make the results particularly susceptible to contamination by common Pb. The presence of common Pb was monitored by using ^{204}Pb, and applying a correction using the measured $^{207}Pb/^{206}Pb$ values for the sample and a common Pb isotopic composition of $^{207}Pb/^{206}Pb = 0.836$ from the average crustal values of Stacey and Kramers (1975). Samples vary in the proportion of ^{206}Pb attributable to common Pb, with the younger units in general having higher percentages. In the younger units these values were often >20%, and cut-offs of common Pb of >30% to >50% were used to exclude analyses with sometimes plausible, but imprecise ages from consideration. The older samples generally had lower proportions of common Pb, and cut-offs of >10% or >20% were used (Table 2).

Table 2: Summary of the U-Pb data

Sample	Number of analyses		Comm. Pb cut-off (%)	Youngest age determinations			
	Total	Viable		Age (Ma)	2 s.d.	MWSD	Prob.
NM2-01	33	30	20	1.88	0.03	1.16	0.30
NM5-01	31	30	40	0.915	0.055	0.66	0.68
NM11-01	41	21	30	0.873	0.031	0.97	0.46
NM3-01	37	36	30	0.806	0.032	0.51	0.68
NM3-02	20	19	50	0.701	0.039	1.04	0.41
RK6-01	33	27	10	1.89	0.02	0.82	0.63

5. RESULTS

Individual ages determined for a single zircon crystal are interpreted to represent a crystallisation age, not necessarily an eruption age. The peaks in the crystallisation age distribution (pdf peaks, as generated in Isoplot) for all zircons in a given sample may predate the eruption ages by tens to hundreds of thousands of years (Wilson et al., 2008). The youngest zircons, therefore, provide a closer approximation for the eruption age. Here, eruption ages are estimated from the weighted mean ages of the younger mode in bi- or polymodal distributions.

5.1 NM2-01

A total of 33 grains were analysed from this sample, three of which have >20 % of ^{206}Pb attributable to common Pb and were excluded from the data set. The age distribution is bimodal, with a pdf peak at 1.93 Ma (Figure 4). The weighted mean of the 16 viable ages in the younger mode is 1.88 ± 0.03 Ma, which is considered to be the best estimate for the eruption age of this unit.

5.2 NM5-01

This sample produced 30 viable analyses containing <40 % of ^{206}Pb attributable to common Pb. The age data show a weakly bimodal distribution, with a pdf peak at ~1.07 Ma (Figure 5). The weighted mean for the 7 grains in the younger mode is 0.915 ± 0.055, which is considered to be the best estimate for the eruption age of this deposit.

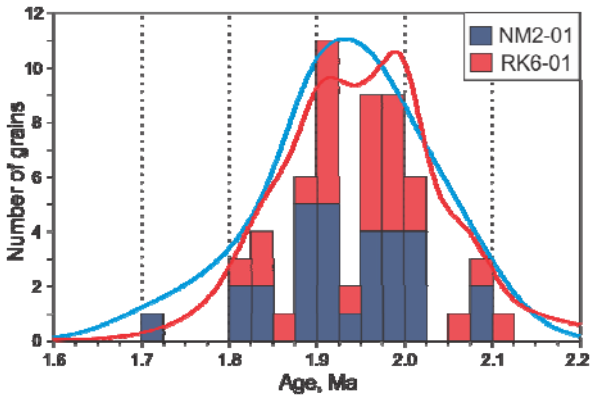

Figure 4: Histograms and probability density curves (created using Isoplot: Ludwig, 2011) for zircons from samples NM2-01 and RK6-01.

5.3 NM11-01

Zircons from this sample generally have low U concentrations, resulting in low count rates, and often have high common Pb values. In order to reduce the uncertainties resulting from these factors, only grains with >180 ppm U and <30% of ^{206}Pb attributable to common Pb have been considered here. The 21 grains that meet these specifications have a bimodal age distribution, with a tail of incorporated grains back to ~2 Ma (Figure 5). The average of the 10 grains in the youngest mode is 0.873 ± 0.031 Ma, which is considered to be the best estimate of the eruption age of this deposit.

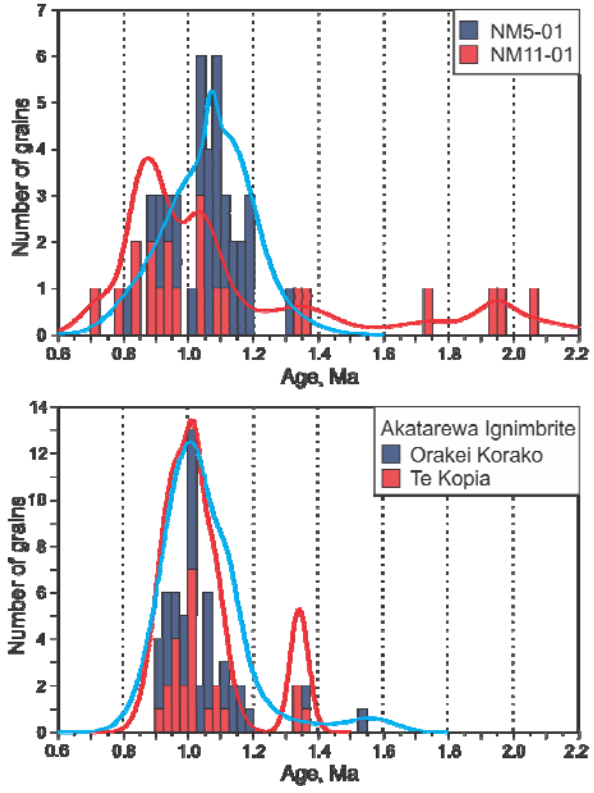

Figure 5: Histograms and probability density curves (created using Isoplot: Ludwig, 2011) for zircons from samples NM5-01 and NM11-01 and the Akatarewa ignimbrite from Orakei Korako and Te Kopia (Wilson et al., 2010).

5.4 NM3-01

Of the 37 grains analysed, one contained >30 % of ^{206}Pb attributable to common Pb and was excluded from the data set. This unit has a very mixed population of zircon ages, with pdf peaks at about 0.80, 0.99, 1.06 and 1.89 Ma, although the majority of grains contribute to the peaks at around 1 Ma (Figure 6). The average of the 4 grains in the youngest peak is 0.806 ± 0.032 Ma, which is considered to be the best estimate for the age of this deposit.

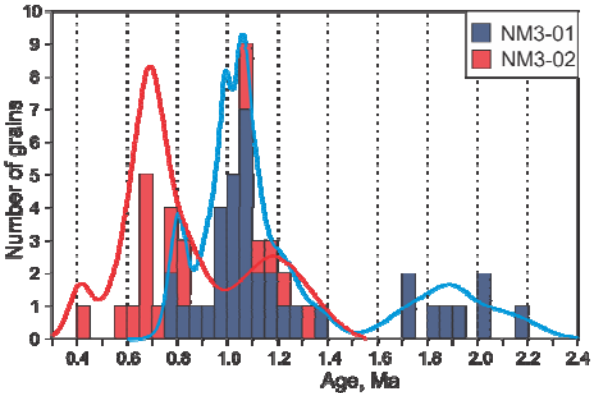

Figure 6: Histograms and probability density curves (created using Isoplot: Ludwig, 2011) for zircons from samples NM3-01 and NM3-02.

5.5 NM3-02

This sample was particularly zircon-poor compared to the other samples presented here, and as a result only a small number of suitable grains were available for analysis. Only 19 viable ages with <30% of ^{206}Pb attributable to common Pb were obtained. There is a dominant pdf peak at 0.7 Ma, with an older peak at 1.2 Ma attributed to inherited grains (Figure 6). A single grain at 0.4 Ma is interpreted to be the result of contamination during sample preparation. The 12 grains in the dominant PDF peak have a weighted mean age of 0.701 ± 0.039 Ma, which is considered the best estimate for the eruption age of this unit.

5.6 RK6-01

Zircons from this sample yielded 27 viable analyses with <10 % of ^{206}Pb attributable to common Pb. The age distribution is weakly bimodal, with peaks shortly after 1.9 Ma and shortly before 2.0 Ma (Figure 4). The weighted mean age for the 13 grains that form the younger mode is 1.89 ± 0.03 Ma, and this is considered the best estimate for the eruption age of this deposit.

6. DISCUSSION

6.1 Correlation of dated Tahorakuri Formation units

Despite the similar age of samples NM2-01 and RK6-01, petrographic characteristics imply that they are separate units. Both are significantly older than any published dates for silicic rocks originating from the TVZ. The ages are closer to the youngest ignimbrite attributed to the Coromandel Volcanic Zone (CVZ), the Upper Papamoa ignimbrite, dated at 1.9 Ma (Briggs et al., 2005). However, a correlation with this ignimbrite, which outcrops over a relatively small area >80 km to the north, must also be doubtful. They are also similar in age to deep Tahorakuri samples from drillholes NM8A (1.85 ± 0.06 Ma) and BR59 (1.83 ± 0.04 Ma: Chambefort et al., 2013). The mineralogy of the NM8A sample differs from both of those from NM2-

01 and RK6-01, implying that multiple units of similar age are present at Ngatamariki and Rotokawa.

Age estimates for samples NM5-01 and NM11-01 overlap within uncertainties, and both have a bimodal age distribution spanning the 1 Ma mark. Both the mineralogy and age data are consistent with both of these samples being the Akatarewa ignimbrite (Figure 5), a welded ignimbrite with a crystal content of 20-25% consisting of plagioclase, quartz, and completely altered ferromagnesian minerals, most likely amphibole based on shape (Bignall et al., 1996). There are no recognised surface exposures of the Akatarewa ignimbrite.

Ignimbrites of a comparable age that are exposed at the surface can be eliminated as correlatives on the basis of their petrographic characteristics. The 0.95 Ma Marshall ignimbrites (Houghton et al., 1995) are crystal-poor with only trace amounts of quartz and no amphibole (Martin, 1961). The 0.89 Ma Tikorangi ignimbrite (Houghton et al., 1995) is quartz-free, and is restricted to limited exposures in the Matahana Basin (Hildyard et al., 2000). The 1.00 Ma Rocky Hill ignimbrite (Houghton et al., 1995) is notable for the abundance of amphibole and the presence of biotite (Martin, 1961; Schipper, 2004), while the 1.01 Ma Kidnappers ignimbrite (Wilson et al., 2009) contains abundant biotite with only trace amounts of quartz (Schipper, 2004).

The youngest pdf peak in sample NM3-01 is similar in age to that of the Waiotapu ignimbrite, which has a pdf peak at ~0.79 Ma (Wilson et al., 2010). However, the Waiotapu ignimbrite has a homogenous zircon age population, and its $^{40}Ar/^{39}Ar$ eruption age estimate of 0.71 ± 0.06 Ma is significantly younger than that estimated here (Houghton et al., 1995). In addition, the Waiotapu ignimbrite is a strongly welded, crystal- and quartz-poor ignimbrite with highly attenuated pumice (Ritchie, 1996). In comparison, NM3-01 contains no obvious welding textures and has a moderate crystal content including quartz. The 0.77 ± 0.03 Ma Rahopaka ignimbrite (Houghton et al., 1995) is similar in age, but is described as a hornblende-rich ignimbrite with a restricted distribution close to its proposed Kapenga caldera source (Murphy and Seward, 1981), making a correlation doubtful.

The mixed zircon population of NM3-01 highlights the possibility that this might not be a primary unit, but instead might be a secondary (re-sedimented) volcaniclastic deposit that has incorporated material from older units. The peaks at around 1 Ma are similar in age to the Akatarewa ignimbrite, while the peak at ~1.9 Ma is similar to the oldest units dated here. Close to 90% of the zircons analysed appear to be related to inheritance from these older deposits. As this sample is intensely altered, primary textures are poorly preserved, and while this sample was initially thought to be a primary ignimbrite, this may not be the case.

The Waiotapu ignimbrite is the only ignimbrite of similar age to sample NM3-02 that outcrops in the TVZ. Both are strongly welded ignimbrites with low crystal contents. However, the zircon age data presented by Wilson et al. (2010) for the Waiotapu ignimbrite is somewhat older, with a pdf peak at 0.79 Ma, almost 100 ka older than the pdf peak for NM3-02. The Waiotapu ignimbrite also has a narrow spectrum of dates, whereas NM3-02 has significant inheritance of zircons. On this basis a correlation to the Waiotapu ignimbrite is uncertain, and the NM3-02 unit may not be exposed at the surface.

6.2 Implications of the U-Pb data

These age data also provide age constraints on thick sequences of andesite beneath the Tahorakuri Formation at Rotokawa. The andesite rests on greywacke basement, and must have formed a sizable composite cone volcano, with known thicknesses of up to 2100 m (Rae, 2007). The andesite must have been emplaced prior to 1.89 Ma, matching the oldest known TVZ andesite cones. Previously the oldest dated andesitic volcanism attributed to the TVZ was found along the western margin at ~2 Ma (Wilson et al., 1995; Figure 1). Our data shows that andesitic volcanism was also occurring close to the eastern margin of the TVZ prior to ~1.9 Ma. This contradicts the notion that andesitic arc volcanism has migrated eastwards across the central North Island over the last ~4 Ma (e.g., Stern, 1987), as andesite along the eastern margin of the TVZ should be considerably younger according to this hypothesis.

The Tahorakuri Formation formed over a period of >1.5 million years, and there is no evidence for thick intra-caldera fill at Ngatamariki or Rotokawa. The depositional record was dominated by pyroclastic rocks for over 1 million years from ~1.9 Ma. Sediments then dominated the depositional record following the emplacement of the youngest pyroclastic deposits at ~0.7 Ma until emplacement of the Whakamaru-group ignimbrites.

In Ngatamariki well NM2, it is not certain how thick the pyroclastic deposits below the 1.88 Ma dated sample are, but similar pyroclastic deposits extend ~550 m deeper in nearby NM8A (Chambefort et al., 2013). No fault that may have down-dropped the deposits in NM8A has been identified, so a significant amount of material ~1.88 Ma or older must be present. Therefore, it does not simply represent a veneer resting on a topographically high area, but must have been deposited in a subsiding basin. In Rotokawa well RK6, ~250 m of the Tahorakuri Formation overlies andesite, with ~100 m between the andesite and the core dated at 1.89 Ma. The presence of such significant thicknesses of silicic deposits overlying what was a relatively large volcano suggests that the onset of subsidence must pre-date emplacement of the Tahorakuri Formation, that is, prior to ~1.9 Ma. This in turn suggests that rifting may have accompanied volcanism throughout the ~2 Ma history of the TVZ. However, it is also possible that the early subsidence is related to activity in the CVZ, and some authors have suggested the likelihood of the CVZ extending beneath the TVZ (e.g., Cole, 1990). Despite this uncertainty, there is good evidence of subsidence in what is now the central TVZ prior to ~1.9 Ma, and the amount of subsidence observed suggests it is related to rifting.

The source(s) of the earliest Tahorakuri Formation pyroclastic deposits cannot be located based on the currently available data. Rifting and silicic volcanism are closely related processes within the present-day TVZ (Gravley et al., 2007; Wilson et al., 2009), and the results presented here suggest that silicic volcanism within the central TVZ may also have begun by ~1.9 Ma. This study and others such as Wilson et al. (2010), Milicich et al. (2013) and Chambefort et al. (2013) show that a significant amount of silicic pyroclastic deposition took place in the TVZ in the period prior to 1 Ma. That rifting likely accompanied this large-scale deposition certainly highlights

the possibility that silicic volcanism was also occurring within the central TVZ very early in its history.

7. CONCLUSION

Samples of the Tahorakuri Formation from Ngatamariki and Rotokawa were dated between 1.89 and 0.70 Ma, highlighting the long time period represented by this formation. The Akatarewa ignimbrite is present at Ngatamariki, with two samples similar in age and mineralogy that dated at Orakei Korako and Te Kopia. No surface deposits of the Akatarewa ignimbrite have been definitively identified in the central TVZ.

Early volcanic activity in the area of Ngatamariki and Rotokawa geothermal fields was andesitic, with a large >1.89 Ma andesitic volcano centred at Rotokawa. This was followed by significant silicic deposition from 1.89 Ma. Rifting of the TVZ also likely began prior to ~1.89 Ma, as shown by thick accumulations of pyroclastic deposits in a subsiding basin at Ngatamariki and Rotokawa.

ACKNOWLEDGEMENTS

This project forms part of the Master's thesis of the senior author, which is funded by the Ministry of Business, Innovation, and Employment's TechNZ scholarship. Logistic funding for this work was provided by the Source to Surface programme and the Mason Trust Fund from the University of Canterbury. Chambefort and Wilson acknowledge support from the Ministry of Business, Innovation and Employment. Additional funding to Chambefort came from GNS Science CSA (Core Science Area) Geothermal Research Programme. Mighty River Power Limited kindly provided access to core sheds and relevant samples and reports.

REFERENCES

Anderson, L.C.A. (2011), A comparison of buried andesites at Ngatamariki and Rotokawa geothermal fields, Taupo, M.Sc. thesis, University of Waikato, Hamilton, New Zealand.

Arehart, G.B., Christenson, B.W., Wood, C.P., Foland, K.A., Browne, P.R.L. (2002), Timing of volcanic, plutonic and geothermal activity at Ngatamariki, New Zealand. Journal of Volcanology and Geothermal Research, 116, 201–214.

Bibby, H.M., Caldwell, T.G., Davey, F.J., Webb, T.H. (1995), Geophysical evidence on the structure of the Taupo Volcanic Zone and its hydrothermal circulation, Journal of Volcanology and Geothermal Research, 68, 29–58.

Bignall, G. (2009), Ngatamariki Geothermal Field geoscience overview, GNS Science consultancy report 2009/94, 41p.

Bignall, G., Browne, P.R.L., Kyle, P.R. (1996), Geochemical characterisation of hydrothermally altered ignimbrites in active geothermal fields from the central Taupo Volcanic Zone, New Zealand, Journal of Volcanology and Geothermal Research, 73, 79–97.

Boseley, C., Cumming, W., Urzúa-Monsalve, L., Powell, T., Grant, M. (2010), A resource conceptual model for the Ngatamariki Geothermal Field based on recent exploration well drilling and 3D MT resistivity imaging, Proceedings of the World Geothermal Congress, Bali, Indonesia.

Briggs, R.M., Houghton, B.F., McWilliams, M., Wilson, C.J.N. (2005), $^{40}Ar/^{39}Ar$ ages of silicic volcanic rocks in the Tauranga-Kaimai area, New Zealand: Dating the transition between volcanism in the Coromandel Arc and the Taupo Volcanic Zone, New Zealand Journal of Geology and Geophysics, 48, 459–469.

Browne, P.R.L., Graham, I.J., Parker, R.J., Wood, C.P. (1992), Subsurface andesite lavas and plutonic rocks in the Rotokawa and Ngatamariki geothermal systems, Taupo Volcanic Zone, New Zealand, Journal of Volcanology and Geothermal Research, 51, 199–215.

Chambefort, I., Lewis, B., Wilson, C.J.N., Bignall, G., Rae, A.J., Coutts, C., Ireland, T.R. (2013), Stratigraphy and structure of the Ngatamariki geothermal system: New U-Pb geochronology and its implications for Taupo Volcanic Zone evolution, Journal of Volcanology and Geothermal Research, under review.

Cole, J.W. (1990), Structural control and origin of volcanism in the Taupo volcanic zone, New Zealand, Bulletin of Volcanology, 52, 445–459.

Graham, I.J., Cole, J.W., Briggs, R.M., Gamble, J.A., Smith, I.E.M. (1995), Petrology and petrogenesis of volcanic rocks from the Taupo Volcanic Zone: a review, Journal of Volcanology and Geothermal Research, 68, 59–87.

Gravley, D.M., Wilson, C.J.N., Rosenberg, M.D., Leonard, G.S. (2006), The nature and age of Ohakuri Formation and Ohakuri Group rocks in surface exposures and geothermal drillhole sequences in the central Taupo Volcanic Zone, New Zealand, New Zealand Journal of Geology and Geophysics, 49, 305–308.

Gravley, D.M., Wilson, C.J.N., Leonard, G.S., Cole, J.W. (2007), Double trouble: Paired ignimbrite eruptions and collateral subsidence in the Taupo Volcanic Zone, New Zealand, Geological Society of America Bulletin, 119, 18–30.

Hildyard, S.C., Cole, J.W., Weaver, S.D. (2000), Tikorangi Ignimbrite: A 0.89 Ma mixed andesite-rhyolite ignimbrite, Matahana Basin, Taupo Volcanic Zone, New Zealand, New Zealand Journal of Geology and Geophysics, 43, 95–107.

Houghton, B.F., Wilson, C.J.N., McWilliams, M.O., Lanphere, M.A., Weaver, S.D., Briggs, R.M., Pringle, M.S. (1995), Chronology and dynamics of a large silicic magmatic system: Central Taupo Volcanic Zone, New Zealand, Geology, 23, 13–16.

Lee, J.M., Townsend, D., Bland, K., Kamp, P.J.J. (compilers) (2011), Geology of the Hawke's Bay area, Institute of Geological & Nuclear Sciences 1:250,000 geological map 8, GNS Science, Lower Hutt, New Zealand.

Leonard, G.S., Begg, J.G., Wilson, C.J.N. (compilers) (2010), Geology of the Rotorua area, Institute of

Geological & Nuclear Sciences 1:250,000 geological map 5, GNS Science. Lower Hutt, New Zealand.

Ludwig, K. (2009), SQUID 2: A User's Manual, revision of 12 April, 2009, Berkeley Geochronology Center Special Publication 5.

Ludwig, K. (2011), Isoplot/Ex version 4.13, a geochronological toolkit for Microsoft Excel, Berkeley Geochronology Centre, Berkeley, California (revision of January 02, 2011).

Martin, R.C. (1961), Stratigraphy and structural outline of the Taupo Volcanic Zone, New Zealand Journal of Geology and Geophysics, 4, 449–478.

Milicich, S.D., Wilson, C.J.N., Bignall, G., Pezaro, B., Charlier, B.L.A., Wooden, J.L., Ireland, T.R. (2013), U–Pb dating of zircon in hydrothermally altered rocks of the Kawerau Geothermal Field, Taupo Volcanic Zone, New Zealand, Journal of Volcanology and Geothermal Research, 253, 97–113.

Murphy, R.P., and Seward, D. (1981), Stratigraphy, lithology, paleomagnetism, and fission track ages of some ignimbrite formations in the Matahana Basin, New Zealand, New Zealand Journal of Geology and Geophysics, 24, 325-331.

Rae, A.J. (2007), Rotokawa geology and geophysics, GNS Science consultancy report 2007/83.

Risk, G.F. (2000), Electrical resistivity surveys of the Rotokawa Geothermal Field, New Zealand, Proceedings of the 22nd New Zealand Geothermal Workshop, 121-126.

Ritchie, A.B.H. (1996), Volcanic geology and geochemistry of Waiotapu Ignimbrite, Taupo Volcanic Zone, New Zealand, M.Sc. thesis, University of Canterbury, Christchurch, New Zealand.

Schärer, U. (1984), The effect of initial ^{230}Th disequilibrium on young U-Pb ages: the Makalu case, Himalaya, Earth and Planetary Science Letters, 67, 191–204.

Schipper, C.I. (2004), Chemical and mineralogical characterization of pyroclastic deposits from the ca. 1 Ma Kidnappers and Rocky Hill eruptions, Taupo Volcanic Zone, New Zealand, M.Sc. thesis, University of Otago, Dunedin, New Zealand.

Stacey, J.S., and Kramers, J.D. (1975), Approximation of terrestrial lead isotope evolution by a two-stage model, Earth and Planetary Science Letters, 26, 207–221.

Stern, T.A. (1987), Asymmetric back-arc spreading, heat flux and structure associated with the Central Volcanic Region of New Zealand, Earth and Planetary Science Letters, 85, 265–276.

Townsend, D., Vonk, A., Kamp, P.J.J. (compilers) (2008), Geology of the Taranaki area, Institute of Geological & Nuclear Sciences 1:250,000 geological map 7. GNS Science. Lower Hutt, New Zealand.

Urzúa-Monsalve, L.A. (2008), MT analysis with geology and geochemistry in a conceptual model of the Ngatamariki Geothermal Field, M.Sc. thesis, University of Auckland, Auckland, New Zealand.

Villamor, P., and Berryman, K.R. (2006), Evolution of the southern termination of the Taupo Rift, New Zealand, New Zealand Journal of Geology and Geophysics, 49, 23–37.

Wallace, L.M., Beavan, J., McCaffrey, R., Darby, D.J. (2004), Subduction zone coupling and tectonic block rotations in the North Island, New Zealand, Journal of Geophysical Research, 109, B12406.

Wilson, C.J.N., Houghton, B.F., Lloyd, E.F. (1986), Volcanic history and evolution of the Maroa-Taupo area, central North Island, Royal Society of New Zealand Bulletin 23, 194-223.

Wilson, C.J.N., Houghton, B.F., McWilliams, M.O., Lanphere, M.A., Weaver, S.D., Briggs, R.M. (1995), Volcanic and structural evolution of Taupo Volcanic Zone, New Zealand: a review, Journal of Volcanology and Geothermal Research, 68, 1–28.

Wilson, C.J.N., Charlier, B.L.A., Fagan, C.J., Spinks, K.D., Gravley, D.M., Simmons, S.F., Browne, P.R.L. (2008), U–Pb dating of zircon in hydrothermally altered rocks as a correlation tool: Application to the Mangakino geothermal field, New Zealand, Journal of Volcanology and Geothermal Research, 176, 191–198.

Wilson, C.J.N., Gravley, D.M., Leonard, G.S., Rowland, J.V. (2009), Volcanism in the central Taupo Volcanic Zone, New Zealand: tempo, styles and controls, Special Publications of IAVCEI, 2, 225–247.

Wilson, C.J.N., Charlier, B.L.A., Rowland, J.V., Browne, P.R.L. (2010), U–Pb dating of zircon in subsurface, hydrothermally altered pyroclastic deposits and implications for subsidence in a magmatically active rift: Taupo Volcanic Zone, New Zealand, Journal of Volcanology and Geothermal Research, 191, 69–78.